Applied Materials Today 29 (2022) 101618

Contents lists available at ScienceDirect

Applied Materials Today

journal homepage: www.elsevier.com/locate/apmt

Modulating noncovalent and covalent forces to control inverse phosphocholine lipid self-assembly on inorganic surfaces: Nanoarchitectonic design principles

Tun Naw Sut [a,b], Abdul Rahim Ferhan [a], Soohyun Park [a], Dong Jun Koo [b], Bo Kyeong Yoon [c], Joshua A. Jackman [b,*], Nam-Joon Cho [a,*]

[a] School of Materials Science and Engineering, Nanyang Technological University, 50 Nanyang Drive, 637553, Singapore
[b] School of Chemical Engineering and Translational Nanobioscience Research Center, Sungkyunkwan University, Suwon 16419, Republic of Korea
[c] School of Healthcare and Biomedical Engineering, Chonnam National University, Yeosu 59626, Republic of Korea

ARTICLE INFO

Keywords:
Supported lipid bilayer
Antifouling
Noncovalent
Coordination chemistry
Interfacial forces

ABSTRACT

While noncovalent forces typically drive lipid vesicle adsorption and rupture to form supported lipid bilayer (SLB) coatings on inorganic surfaces for various material science applications, this strategy only works on a few materials with suitable energetics such as SiO_2. The use of coordination chemistry between inverse phosphocholine (PC) lipid headgroups and surfaces has emerged as a promising strategy to enable SLB formation on other materials such as TiO_2 based on covalent forces. However, until now, a cohesive picture of how noncovalent and covalent forces jointly contribute to the SLB formation process on TiO_2 has been lacking and addressing this gap is important to design functional lipid biointerfaces with tailored properties such as antifouling capabilities. Herein, we investigated inverse PC lipid vesicle adsorption onto TiO_2 and SiO_2 surfaces and discovered how adsorption pathways can be controlled by tuning the balance of noncovalent and covalent forces, which enabled us to establish molecular design rules to fabricate physically robust SLB coatings on macroscopically flat TiO_2 surfaces. On TiO_2, SLB formation depended on two key factors: (1) favorable noncovalent forces to facilitate initial vesicle adsorption; and (2) a critical density of lipid-TiO_2 covalent bonds to enable sufficient vesicle deformation triggering fusion and rupture. In other cases, either no adsorption or intact vesicle adsorption without rupture occurred even when covalent bonds were present. Conversely, on SiO_2, conditions were identified to support inverse PC lipid adsorption whereas vesicles were repelled otherwise. The experimental results were supported by interfacial force modeling and our findings demonstrate how a subtle interplay of noncovalent and covalent forces plays a deterministic role in modulating lipid self-assembly pathways. Specific conditions in which the physically stable, fabricated SLBs on TiO_2 surfaces exhibit antifouling properties were also identified based on optimizing the lipid composition to enhance vesicle-surface interactions while preventing other nonspecific interaction events.

1. Introduction

Understanding how phospholipid membranes interact with inorganic materials is critical to various applications such as biosensors and drug delivery tools, and can enable the design of functional biointerfaces such as ultrathin supported lipid bilayer (SLB) coatings [1–3]. SLBs are usually composed of naturally occurring, biocompatible phosphatidylcholine (PC) lipids as the main component and can impart antifouling properties as well as aid selective biofunctionalization [4,5]. Such efforts fit within the nanoarchitectonics concept to control the molecular self-assembly of phospholipids with a defined nanoscale organization at a solid-liquid interface [6,7]. The most common approach to SLB fabrication involves the noncovalent adsorption and spontaneous rupture of nanoscopic lipid vesicles at solid-liquid interfaces [8–12]. Interestingly, this self-assembly process can only occur on a narrow range of surfaces with favorable material properties and mechanistic details continue to be unraveled through experimental, simulation, and theoretical approaches [12–15]. There is extensive interest in

* Corresponding authors.
E-mail addresses: jjackman@skku.edu (J.A. Jackman), njcho@ntu.edu.sg (N.-J. Cho).

https://doi.org/10.1016/j.apmt.2022.101618
Received 18 June 2022; Received in revised form 29 July 2022; Accepted 7 August 2022
Available online 23 August 2022

deciphering why lipid vesicles adsorb and rupture on certain hydrophilic surfaces, but not others, and translating such chemical insights into the design of improved SLB biointerfaces with tailored properties and stabilities.

The prevailing notion is that zwitterionic PC lipid vesicles can adsorb and rupture spontaneously on SiO_2 surfaces to form an SLB coating while they typically adsorb and remain intact on TiO_2 surfaces [16]. The distinct self-assembly outcomes are believed to arise from differences in vesicle-surface interaction strength [17–20]. On SiO_2, adsorbed PC lipid vesicles undergo more extensive deformation due to stronger vesicle-surface interactions, which makes them more prone to fusion and rupture [20]. Conversely, adsorbed vesicles have weaker interactions with TiO_2 surfaces, resulting in less deformation [21]. The different extents of vesicle deformation have been measured experimentally [22] (see also related work on SLB systems [23]) and the surface-dependent variation in vesicle-surface interactions has also been discussed in the context of noncovalent interfacial forces, including van der Waals, double-layer electrostatic, and steric-hydration forces [24]. To fabricate SLBs on TiO_2 surfaces, there have also been efforts to enhance vesicle-surface interactions by virtue of changing solution pH to adjust the TiO_2 surface charge [25] and by using positively charged lipid vesicles in place of conventionally used zwitterionic lipid vesicles, in which case strong electrostatic attraction can drive vesicle fusion and rupture [26]. An interesting extension of the latter approach involves lipid transfer between a pre-fabricated, positively charged SLB and phosphatidylserine (PS)-containing lipid vesicles, which can result in an SLB that consists of a mixture of positively and negatively charged lipids. It is also possible to directly utilize vesicles that contain negatively charged PS lipids in the presence of divalent cations, which act as a bridge to facilitate attractive lipid-TiO_2 interactions [27]. Alternative approaches that bypass the need for deformation-mediated vesicle rupture like solvent-exchange processes have additionally been reported [28,29].

The aforementioned efforts have relied on noncovalent strategies that typically result in weakly attached SLBs while there have also been creative strategies to fabricate SLB coatings on TiO_2 surfaces by utilizing coordination chemistry — a line of research that not only has practical utility but also sheds light on the fundamental chemistry of phospholipid membranes on inorganic surfaces [30]. These strategies have been centered around inverse PC lipids, which are structurally similar to PC lipids but have a flipped headgroup whereby the quaternary amine is connected to the glycerol backbone and the anionic phosphate group is presented outward [31]. The main example of an inverse PC lipid is 2-((2,3-bis(oleoyloxy)propyl)dimethylammonio)ethyl hydrogen phosphate (DOCP) and negatively charged DOCP lipid vesicles have been reported to spontaneously fuse with TiO_2 nanoparticles to form covalently attached SLB coatings [32,33].

Strikingly, DOCP lipid vesicles do not fuse with SiO_2 nanoparticles, which is an opposite trend to that observed with zwitterionic PC lipid vesicles that fuse with SiO_2, but not TiO_2, nanoparticles [32]. The distinct interaction behavior of DOCP lipid vesicles with TiO_2 nanoparticles has been attributed to coordination between the phosphate moiety of the DOCP headgroup and titanium atoms, which results in covalent P-O-Ti bond formation [34] and enhances vesicle-surface interactions on TiO_2 surfaces, whereas DOCP lipid vesicles are generally repelled from SiO_2 surfaces [35]. It has also been shown that DOCP lipid vesicles can fuse with TiO_2 nanoparticles across a wide range of pH conditions, reinforcing the importance of covalent bond formation while the inability of DOCP lipid vesicles to fuse with SiO_2 nanoparticles has been attributed to charge repulsion [35]. As such, existing efforts have viewed covalent and noncovalent forces as discrete factors in driving DOCP lipid vesicle interactions with TiO_2 and SiO_2 surfaces, respectively. However, this mechanistic picture is likely incomplete, especially in the TiO_2 case, as it is known that noncovalent forces play a universally important role in vesicle-surface adhesion processes. Hence, there is an outstanding need to unify the mechanistic picture of how noncovalent interfacial forces and coordination chemistry contribute to DOCP lipid vesicle interactions with inorganic surfaces.

Towards this goal, herein, we scrutinized the real-time adsorption kinetics of ~70 nm diameter, DOCP-containing lipid vesicles onto flat, macroscopic TiO_2 and SiO_2 surfaces and unraveled how the interplay of noncovalent and covalent forces in this system plays a deterministic role in modulating self-assembly pathways. While coordination chemistry has been viewed as a critical factor in enabling DOCP-containing lipid vesicles to fuse with and form SLBs on TiO_2 surfaces, our findings reveal a more nuanced situation whereby noncovalent forces mediate initial adsorption and a minimum density of covalent bonds between vesicles and the surface must form to enable a sufficiently high degree of vesicle deformation that leads to vesicle fusion and rupture. We also investigate functional properties of the resulting SLBs that are pertinent to defining the scope of suitable material science applications.

2. Materials and methods

2.1. Materials

Chloroform solutions of 2-((2,3-bis(oleoyloxy)propyl)dimethylammonio)ethyl hydrogen phosphate (DOCP), 1,2-dioleoyl-*sn*-glycero-3-phosphocholine (DOPC), and 1,2-dioleoyl-*sn*-glycero-3-phosphoethanolamine-N-(lissamine rhodamine B sulfonyl) (ammonium salt) (Rh-PE) lipids were obtained from Avanti Polar Lipids (Alabaster, AL, USA). All solutions were prepared using Milli-Q-treated water (>18 MΩ·cm) from MilliporeSigma (Burlington, MA, USA). All other reagents and chemicals were purchased from Sigma-Aldrich (St. Louis, MO, USA) unless otherwise specified.

2.2. Vesicle preparation

Lipid vesicles were prepared by the extrusion method, as previously described [36]. The appropriate amount of DOCP and/or DOPC lipids, along with fluorescently labeled 0.5 mol% Rh-PE lipid for fluorescence recovery after photobleaching (FRAP) experiments, in chloroform was dispersed in a glass vial and the solvent was evaporated with a gentle stream of nitrogen gas. The resulting dry lipid film was stored in a vacuum desiccator overnight and then hydrated at a stock concentration of 5 mg/mL in 10 mM Tris buffer [pH 7.5] with 150 mM NaCl concentration. A Mini-Extruder device (Avanti Polar Lipids) was used to extrude the vesicles through a polycarbonate membrane with 50 nm diameter pores. The size distribution of the extruded vesicles was characterized using a 90Plus particle size analyzer (Brookhaven Instruments, Holtsville, NY) and the zeta potential value of the extruded vesicles (diluted in 10 mM Tris buffer [pH 7.5] with 10 mM NaCl) was measured using a Malvern Zetasizer ZS2000 (Malvern Instruments, Malvern, UK). The mean diameter of the vesicle populations was ~70 nm (see Supplementary Table 1). Before QCM-D and FRAP experiments, the vesicles were diluted to 0.1 mg/mL in the appropriate buffer solution.

2.3. Quartz crystal microbalance-dissipation (QCM-D)

Vesicle adsorption kinetics and corresponding adlayer properties were analyzed using a Q-Sense E4 instrument (Biolin Scientific AB, Gothenburg, Sweden). The basic operating principles are described in Ref. [37]. The QCM-D sensor chips were commercially supplied from Biolin Scientific AB and had 50 nm thick, sputter-coated TiO_2 or SiO_2 surfaces. The fundamental resonance frequency of the sensor chips was 5 MHz and the mass sensitivity constant was 17.7 ng cm^{-2} Hz^{-1}. Before experiment, the sensor chips were rinsed with water and ethanol, dried with nitrogen gas, and treated with oxygen plasma for 3 min (TiO_2) or 1 min (SiO_2) by using an Expanded Plasma Cleaner (PDC-002, Harrick Plasma, Ithaca, NY, USA). Liquid samples were injected into the measurement chambers at a volumetric flow rate of 50 μL/min by a

peristaltic pump (Reglo Digital MS-4/6, Ismatec, Glattbrugg, Switzerland). The measurement data were collected using the Q-Soft software program (Biolin Scientific AB) and the reported data correspond to the 5th overtone and were normalized according to the overtone number.

3. Results

3.1. Measurement strategy

We utilized the quartz crystal microbalance-dissipation (QCM-D) technique to characterize the nanoscale mass and viscoelastic properties of lipid adlayers that formed on the TiO_2- and SiO_2-coated sensor surfaces and the corresponding adsorption kinetics could be temporally tracked based on the simultaneously recorded resonance frequency (Δf) and energy dissipation (ΔD) measurement signals, respectively [37]. This label-free characterization method allowed us to directly probe DOCP lipid interactions with inorganic surfaces in real-time, complementing past nanoparticle studies [32,33,35] that mainly focused on measuring fluorescent dye release from within vesicles and dye attached to phospholipids that indirectly inferred vesicle fusion behavior and lipid attachment, respectively.

3.2. Ionic strength effects

Using the QCM-D technique, we first measured 100 mol% DOCP lipid vesicle adsorption onto TiO_2 and SiO_2 surfaces in 10 mM Tris buffer [pH 7.5] with different NaCl concentrations, which mainly influenced the degree of electrostatic interactions based on charge screening and hence modulated the overall degree of noncovalent forces in the system. On TiO_2 surfaces, the Δf and ΔD signals indicated that vesicles adsorbed in 100 mM and higher NaCl concentrations with two-step kinetics, whereas nearly negligible adsorption occurred in 50 mM NaCl (Fig. 1a). The corresponding final Δf and ΔD shifts of the lipid adlayers formed in 100–250 mM NaCl conditions were around -24–-26 Hz and less than 0.3×10^{-6}, respectively, which indicate SLB formation [8] (Fig. 1b). Together, these QCM-D measurement responses are consistent with vesicle adsorption and spontaneous rupture on the TiO_2 surface.

In marked contrast, the final Δf and ΔD shifts of the lipid adlayer formed in the 50 mM NaCl condition were only around -6 Hz and less than 0.3×10^{-6}, respectively, which point to nearly negligible adsorption. Hence, DOCP lipid vesicle adsorption onto TiO_2 surfaces led to SLB formation in 100–250 mM NaCl conditions and there was minimal adsorption in the 50 mM NaCl condition (Fig. 1c). While the phosphate moieties of the DOCP lipid headgroups are known to readily form covalent bonds with the TiO_2 surface *via* coordination [35], the observed dependence on NaCl concentration supports that noncovalent vesicle-surface interactions play a critical role in controlling the initial adsorption process. Since the DOCP lipid vesicles and TiO_2 surface are both negatively charged at pH 7.5 [25,31], these findings further support that salt-mediated charge screening modulates the degree of electrostatic repulsion between contacting vesicles and the surface.

On the other hand, on SiO_2 surfaces, there was negligible DOCP lipid vesicle adsorption at all tested NaCl conditions (Fig. 1d). The corresponding final Δf and ΔD shifts were less than -4 Hz and 0.3×10^{-6}, respectively, which indicate minimal adsorption (Fig. 1e). Since the SiO_2 surface is also negatively charged at pH 7.5 [25], this finding supports that there is a relatively larger degree of electrostatic repulsion between DOCP lipid vesicles and the SiO_2 surface. The lack of vesicle adsorption on the SiO_2 surface also agrees well with a past study that showed DOCP lipid vesicles had low adsorption onto SiO_2 nanoparticles in the 0–100 mM NaCl concentration range [32]. Hence, the results support that DOCP lipid vesicles do not adsorb onto the SiO_2 surface across the tested NaCl concentration range (Fig. 1f).

To complement the QCM-D experiments, we performed analytical calculations to estimate how the noncovalent interfacial forces that

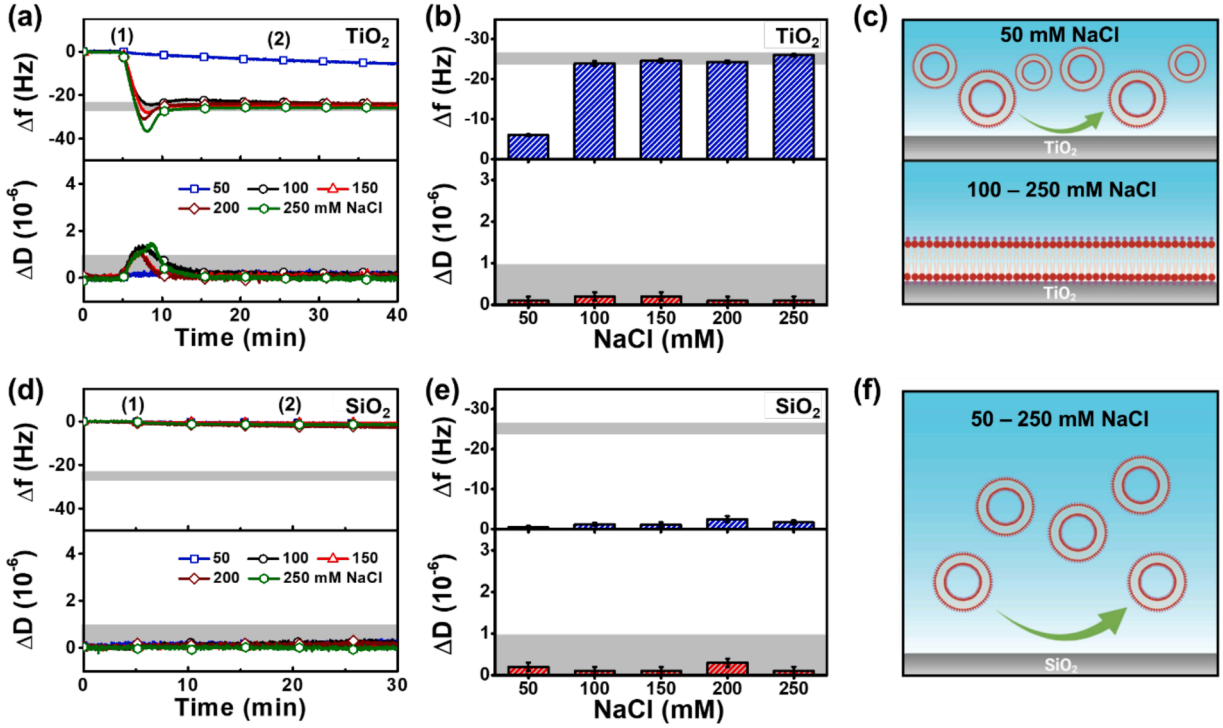

Fig. 1. Effect of NaCl concentration on DOCP lipid vesicle adsorption onto TiO_2 and SiO_2 surfaces. (a) QCM-D frequency (Δf) and energy dissipation (ΔD) signals upon DOCP lipid vesicle addition to TiO_2 surface. Labels 1 and 2 refer to vesicle addition and buffer washing, respectively. (b) Summary of final Δf and ΔD shifts for adsorbed lipid layers on TiO_2 surface. Mean and standard deviation are reported from at least three measurements. Shaded regions in the graphs indicate typical measurement values for an SLB. (c) Illustration of vesicle adsorption outcomes on TiO_2 surface. (d–f) Corresponding data and illustration for DOCP lipid vesicle addition to SiO_2 surface.

underpin DOCP lipid vesicle-surface attachment are influenced by NaCl concentration trendwise. The calculations modeled the vesicle-surface contact region as a planar lipid bilayer on top of a flat surface and considered the van der Waals, double-layer electrostatic, and steric-hydration forces according to extended-DLVO (E-DLVO) theory [38, 39]. The TiO_2 and SiO_2 surfaces as well as the vesicles are negatively charged in our system so the vesicle-surface interaction strength depends on the balance between the attractive van der Waals force and the repulsive electrostatic and steric-hydration forces. These three forces are operative in the low NaCl concentration regime while the magnitude of the electrostatic force becomes appreciably smaller in the high NaCl concentration regime due to charge shielding. In the latter case, the balance mainly depends on the attractive van der Waals force and the repulsive steric-hydration force. In our E-DLVO model analysis, across the range of experimentally tested NaCl concentrations, the vesicle-surface interaction energy was plotted as a function of the separation distance between the vesicle and surface in order to identify the minimum interaction energy, which corresponded to an equilibrium separation distance [39].

In the TiO_2 case, the plots showed that there were attractive interactions between DOCP lipid vesicles and the TiO_2 surface for 100 mM and higher NaCl concentrations, as indicated by stable energy minima at around 2 nm separation distance (Fig. 2a). On the other hand, the calculations showed that there was only a weak interaction between the DOCP lipid vesicles and the TiO_2 surface in the 50 mM NaCl case, which agrees well with the experimental result indicating negligible adsorption (*cf.* Fig. 1). Trendwise, the minimum interaction energy became more favorable and shifted from around -20 to -36 μJ/m^2 as the NaCl concentration increased from 100 to 250 mM, whereas the minimum interaction energy was almost negligible at around -4 μJ/m^2 in the 50 mM NaCl case (Fig. 2b). Note that the magnitude of the maximum E-DLVO interaction energy is around 36 μJ/m^2 (*cf.* Fig. 2a), which is equivalent to 2.6 k_BT/nm^2 where k_B is the Boltzmann constant and T is the temperature (in Kelvin units). For 70-nm diameter vesicles with, e.g., a vesicle-surface contact area on the order of $\pi R^2 = 3847$ nm^2 ($R = 35$ nm is the vesicle radius), the vesicle-surface interaction energy corresponds to around 10,000 k_BT.

In addition, in the SiO_2 case, the plots indicated that there were negligible interactions between DOCP lipid vesicles and the SiO_2 surface across the tested range of NaCl concentrations, which is consistent with the experimental results (Fig. 2c). The interaction energy tended to marginally increase at higher NaCl concentrations due to charge screening, however, the minimum interaction energy was always smaller than -4 μJ/m^2 and hence nearly negligible in all cases (Fig. 2d). In general, the trend in interaction energies obtained from the calculations agreed well with the experimental results for the TiO_2 and SiO_2 cases, supporting that the interplay of noncovalent interfacial forces captured in the analytical model plays an important role in modulating DOCP lipid vesicle-surface interactions on both surfaces. Hence, while DOCP lipid vesicle interactions with inorganic surfaces, especially TiO_2, are typically analyzed in terms of covalent bond formation, these findings establish that noncovalent interactions are a critical factor in dictating vesicle-surface adsorption behavior in this system.

3.3. *Effect of DOCP fraction on vesicle-TiO_2 interactions*

Guided by these observations, we proceeded to investigate how the molar fraction of DOCP lipids within DOCP/DOPC lipid vesicles affects

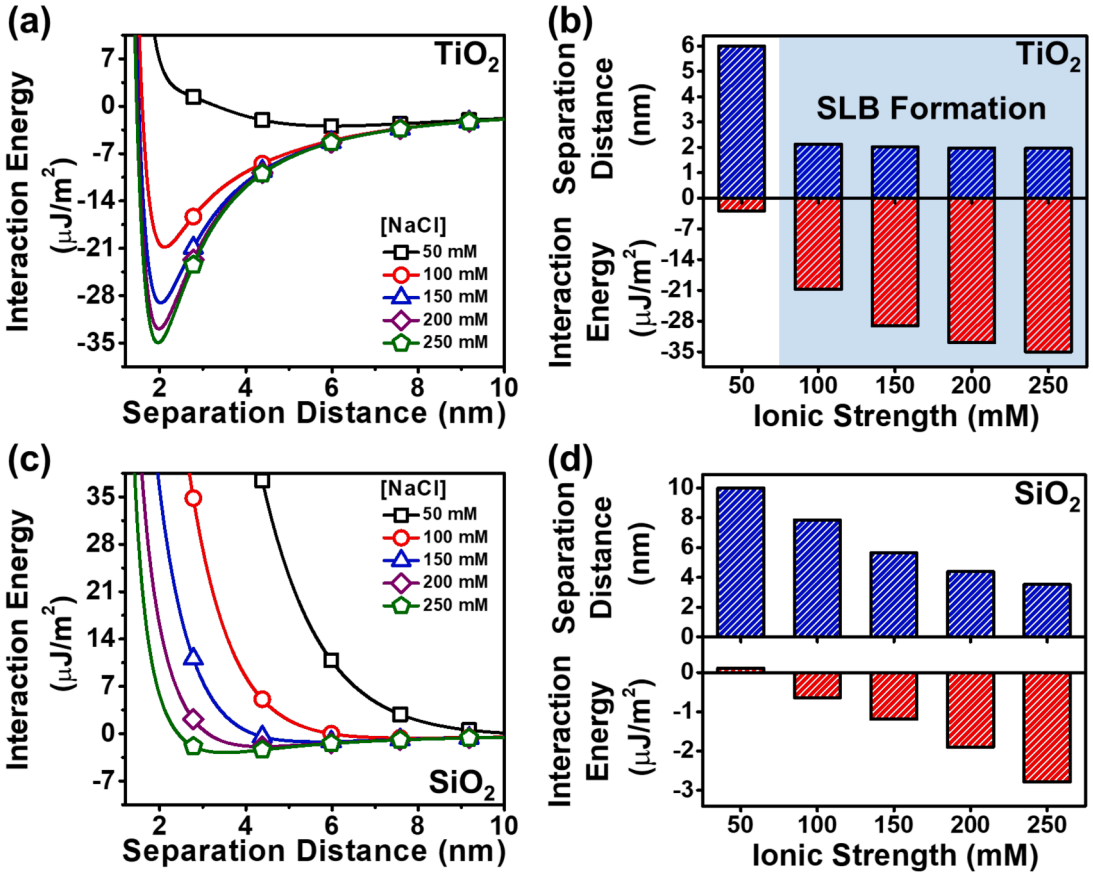

Fig. 2. Extended-DLVO model analysis of DOCP lipid vesicle interactions with TiO_2 and SiO_2 surfaces. (a) Dependence of the total interaction energy on the vesicle-surface separation distance for different NaCl concentrations. (b) Summary values of equilibrium separation distance and interaction energy for adsorbed vesicles on a TiO_2 surface. Shaded region corresponds to NaCl concentrations at which a DOCP SLB formed. (c,d) Corresponding data for adsorbed vesicles on an SiO_2 surface.

adsorption behavior. Past studies have exclusively tested 100 mol% DOCP lipid vesicles and we hypothesized that adjusting the DOCP lipid fraction can modulate self-assembly outcomes by virtue of balancing the interplay of noncovalent and covalent forces involved in vesicle-surface interactions. In these experiments, the buffer solution consisted of 10 mM Tris [pH 7.5] with 150 mM NaCl in all cases and we selected DOPC as the second lipid component because it has a zwitterionic headgroup and the same chain properties as DOCP, i.e., two oleoyl chains, to facilitate fluid-phase mixing of the two lipids in the vesicles and similar membrane mechanical properties.

On TiO_2 surfaces, the QCM-D Δf and ΔD signals showed that DOCP/DOPC lipid vesicles containing 100/0, 75/25, and 50/50 molar fractions adsorbed and exhibited two-step adsorption behavior consistent with spontaneous rupture and SLB formation (Fig. 3a and b). The observed adsorption kinetics are consistent with intact vesicle adsorption, followed by rupture commencing after a critical surface coverage of adsorbed vesicles is reached. Hence, both vesicle-surface and vesicle-vesicle interactions are necessary to facilitate SLB formation, indicating that DOCP-TiO_2 interactions by themselves are insufficient to trigger vesicle rupture. As the DOCP lipid fraction decreased from 100 to

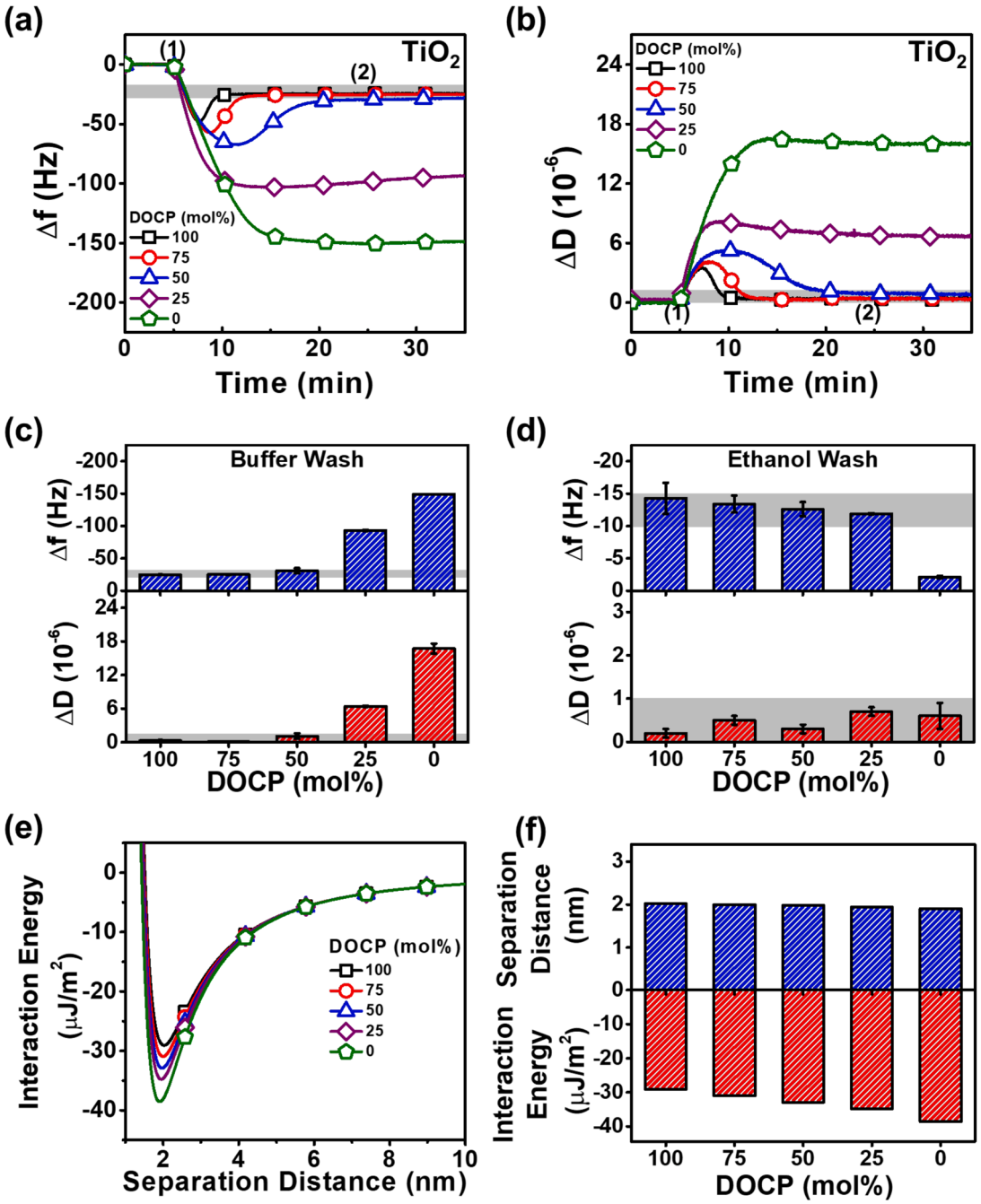

Fig. 3. Tuning DOCP lipid fraction to modulate vesicle adsorption pathway on TiO_2 surface. (a,b) QCM-D frequency (Δf) and energy dissipation (ΔD) signals upon DOCP/DOPC lipid vesicle addition to TiO_2 surface. Labels 1 and 2 refer to vesicle addition and buffer washing, respectively. Summary of final Δf and ΔD shifts after (c) buffer washing and (d) ethanol washing for adsorbed lipid layers on TiO_2 surface. All reported shifts were recorded in buffer solution and are relative to the initial buffer baseline. Mean and standard deviation are reported from at least three measurements. Shaded regions in the graphs indicate typical measurement values for an SLB and lipid monolayer in panels (a–c) and (d), respectively. (e) Dependence of the total interaction energy on the vesicle-surface separation distance according to extended-DLVO model analysis. (f) Summary values of equilibrium separation distance and interaction energy.

50 mol%, the corresponding Δf and ΔD inflection points had larger magnitudes, supporting that a greater surface coverage of adsorbed vesicles and hence more vesicle-vesicle interactions were necessary to induce spontaneous rupture [11,40]. This trend implies that vesicle-surface interactions became weaker at lower DOCP fractions in spite of less charge repulsion, supporting that there was less covalent bond formation between vesicles and the surface (Supplementary Fig. 1). Strikingly, when the DOCP lipid fraction was reduced to 25 mol %, the lipid vesicles adsorbed monotonically but did not rupture on the TiO_2 surface. Control experiments were also performed with 100 mol% DOPC lipid vesicles (0 mol% DOCP), which also adsorbed but did not rupture as expected [16].

For lipid vesicles containing 75–100 mol% DOCP, the corresponding final Δf and ΔD shifts after buffer washing were around -24–-26 Hz and less than 1×10^{-6}, respectively, which indicate SLB formation (Fig. 3c). Similar results were obtained with lipid vesicles containing 50 mol% DOCP, however, the final Δf and ΔD shifts were modestly larger in that case due to incomplete rupture [37]. On the other hand, for lipid vesicles containing 25 mol% DOCP, the final Δf and ΔD shifts after buffer washing were around -100 Hz and 7×10^{-6}, respectively, which is consistent with intact vesicle adsorption [41]. Likewise, for DOPC lipid vesicles, the final Δf and ΔD shifts were around -150 Hz and 16×10^{-6}, respectively, also indicating intact vesicle adsorption while the ratios of Δf/ΔD shift values support that 25/75 DOCP/DOPC lipid vesicles underwent greater adsorption-related deformation than DOPC lipid vesicles [16] (Supplementary Fig. 2). Considering that the 25/75 DOCP/DOPC lipid vesicles are more negatively charged than DOPC lipid vesicles, the greater extent of deformation in the former case supports that covalent DOCP lipid anchoring to the TiO_2 surface *via* coordination enhances vesicle-surface interactions compared to noncovalent interactions alone. Moreover, the observed dependence on DOCP lipid fraction supports that a critical density of DOCP-TiO_2 anchoring sites is needed to trigger vesicle fusion/rupture and SLB formation.

After lipid attachment to the TiO_2 surface, an ethanol washing step was performed to remove noncovalently adsorbed lipid molecules and, after subsequently exchanging back to the buffer solution, the final Δf and ΔD shifts were around -10–-15 Hz and $< 1 \times 10^{-6}$, respectively, for DOCP-containing lipid vesicles relative to the initial buffer baseline (Fig. 3d). This result supports that covalently attached DOCP lipid molecules remained adhered to the TiO_2 surface and formed a monolayer based on the surface mass density (~220 ng/cm^2) according to the Sauerbrey relationship [41]. By contrast, the corresponding Δf and ΔD shifts were only around −2 and $< 1 \times 10^{-6}$, respectively, in the case of DOPC lipid vesicles, which is consistent with the removal of noncovalently adsorbed DOPC lipid molecules from the TiO_2 surface due to ethanol washing. Analytical calculations based on the E-DLVO model further showed that, for all tested lipid compositions, the noncovalent lipid-surface interactions were attractive (at least -25 μJ/m^2) and tended to become more favorable with increasing DOPC lipid fraction due to a lower vesicle surface charge (Fig. 3e and f). Hence, noncovalent interactions played an important role in modulating initial lipid vesicle adsorption onto the TiO_2 surface while covalent interactions involving DOCP lipids were necessary to induce a sufficiently high degree of adsorption-related vesicle deformation that could trigger fusion/rupture and SLB formation [11]. Importantly, a critical density of DOCP-TiO_2 bonding events was necessary to induce SLB formation whereas intact vesicle adsorption without rupture occurred in other cases.

Within the range of lipid compositions that formed SLBs, we also investigated potential antifouling properties. Indeed, as mentioned in the Introduction, zwitterionic PC lipids are the main component that endows SLBs with antifouling properties and we therefore sought to investigate how the presence of negatively charged DOCP lipids in the SLB might influence antifouling properties. Accordingly, using the QCM-D technique, we evaluated the nonspecific adsorption of bovine serum albumin (BSA) protein – a highly abundant protein found in blood – onto fabricated DOPC/DOCP SLBs containing varying DOCP fractions, which were prepared on TiO_2 surfaces. In the case of SLBs containing 75–100 mol% DOCP, BSA adsorbed appreciably whereas there was negligible adsorption onto SLBs that contained 50 mol% DOCP SLBs, which was comparable to results obtained using a 100 mol% DOPC SLB on an SiO_2 surface (Supplementary Fig. 3). Hence, there is an optimal range of lipid compositions, namely the 50/50 mol% DOPC/DOCP lipid composition, that enables SLB fabrication on TiO_2 surfaces by virtue of DOCP lipid anchoring while also maintaining antifouling properties.

Considering that DOCP-TiO_2 covalent bonds act like anchoring points, we further considered how lateral lipid mobility in the fabricated SLBs might be impacted by performing fluorescence recovery after photobleaching (FRAP) experiments (Supplementary Fig. 4). For these experiments, we fabricated a 100 mol% DOCP SLB on a TiO_2 surface, removed the upper leaflet by ethanol washing, and then added 99.5 mol % DOPC lipid vesicles containing 0.5 mol% Rh-PE lipids onto the remaining DOCP monolayer. This protocol resulted in the formation of a DOCP/DOPC SLB that had a fluorescently labeled DOPC upper leaflet on top of a DOCP lower leaflet, which represented a model composition that might be used for applications. We also directly prepared a fluorescently labeled DOCP/DOCP SLB on a TiO_2 surface by using 99.5 mol% DOCP lipid vesicles that contained 0.5 mol% Rh-PE lipid.

The FRAP measurements indicated that the corresponding mobile lipid fractions were around 50 and 75% for DOCP/DOCP and DOCP/DOPC SLBs, respectively. The diffusion coefficients of lateral lipid mobility were around 0.61 ± 0.09 μm^2/s for the DOCP/DOCP SLB and 0.84 ± 0.05 μm^2/s for the DOCP/DOPC SLB. These values are appreciably lower than the typical diffusion coefficient values of around 2.2 μm^2/s for a fluidic DOPC SLB on a SiO_2 surface [42], supporting that the anchoring DOCP lipids in the bottom leaflet are the main contributors to the mobility reduction while the upper leaflet retains a modest degree of mobility, slightly more so after exchanging the upper leaflet to DOPC lipids. These findings support that the DOCP-containing SLBs are firmly attached to the TiO_2 surface, which is also consistent with the mechanistic picture of how a minimum number of anchoring points – as influenced by the DOCP lipid fraction in the precursor vesicles – is needed to drive a sufficiently high degree of vesicle deformation as part of the vesicle rupture process. Furthermore, the findings reinforce that the resulting SLBs are particularly well suited for applications such as molecular diagnostics where the precise surface functionalization (e.g., as enabled by tuning the lipid composition), conformal character, and antifouling properties of the lipid membrane are the main desired features as opposed to applications that require the lipids in the SLB to be mobile for functional purposes, such as biophysical platforms to study receptor-mediated clustering.

3.4. *Effect of DOCP fraction on vesicle-SiO_2 interactions*

Similar composition-dependent experiments were performed on SiO_2 surfaces and the QCM-D results showed that DOCP/DOPC lipid vesicles containing 100/0, 75/25, and 50/50 molar fractions did not adsorb onto the surface (Fig. 4a and b). By contrast, DOCP/DOPC lipid vesicles containing 25 mol% DOCP underwent monotonic adsorption while DOPC lipid vesicles exhibited two-step adsorption behavior that indicated SLB formation. For lipid vesicles containing 50–100 mol% DOCP, the corresponding final Δf and ΔD shifts after buffer washing were less than -2 Hz and 0.5×10^{-6}, respectively, which are consistent with negligible adsorption (Fig. 4c). For 25/75 DOCP/DOPC lipid vesicles, there was modest lipid adsorption that did not result in SLB formation, as indicated by final Δf and ΔD shifts of around -26 Hz and 2×10^{-6}, respectively, whereas DOPC lipid vesicles fused and ruptured to form an SLB with final Δf and ΔD shifts of around -26 Hz and 0.2×10^{-6}, respectively.

After ethanol washing, the Δf and ΔD shifts became fully negligible in the case of lipid vesicles containing 50–100 mol% DOCP (Fig. 4d). On the other hand, for 25/75 DOCP/DOPC lipid vesicles, the final Δf and ΔD shifts were around -15 Hz and 2×10^{-6}, respectively, indicating that

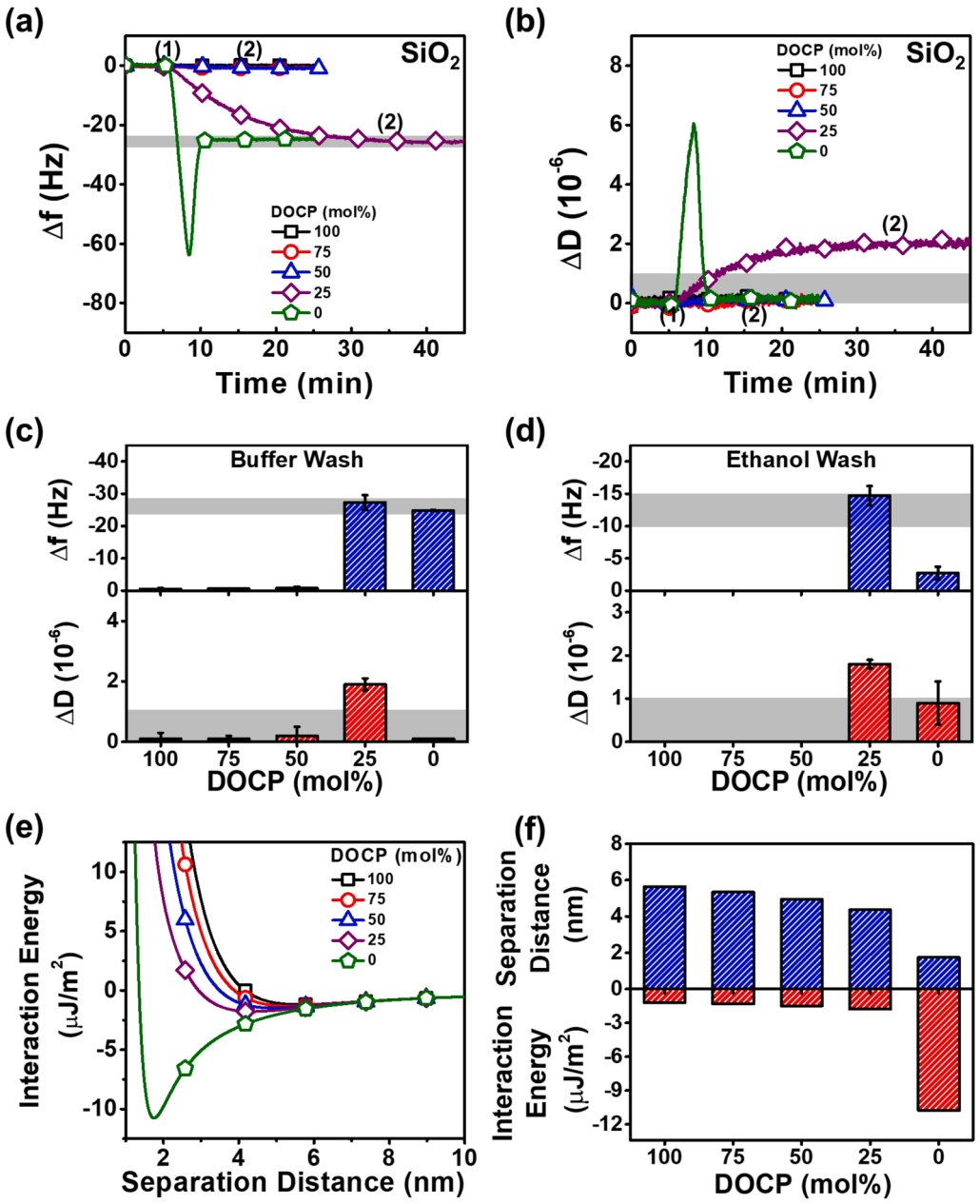

Fig. 4. Tuning DOCP lipid fraction to modulate vesicle adsorption pathway on SiO_2 surface. As in Fig. 3, except that the substrate was SiO_2.

a lipid monolayer remained attached to the surface. Interestingly, this observation supports that DOCP lipids can interact with SiO_2 surfaces provided that the DOCP lipid fraction is sufficiently low so that non-covalent vesicle-surface interactions – arising from reduced charge repulsion and likely involving strong hydrogen-bonding interactions between phosphate groups and silanol (Si-O) groups [43,44] – are favorable enough to permit initial vesicle attachment (see also another example of tight binding of phosphoinositide lipids to SiO_2 surfaces [45]). Conversely, for DOPC lipid vesicles, the final Δf and ΔD shifts were reduced to around -2 Hz and 1×10^{-6}, respectively, which indicate that ethanol washing removed noncovalently attached DOPC lipids from the surface as expected. Furthermore, E-DLVO-based analytical calculations verified that the lipid-surface interaction energy due to non-covalent interactions was very weak for DOCP-containing lipid vesicles on SiO_2 surfaces in general and were more favorable for DOPC lipid vesicles (Fig. 4e and f). These findings are consistent with electrostatic repulsion between negatively charged DOCP-containing lipid vesicles and the SiO_2 surface, which hinders rupture-induced SLB formation even in cases where moderate adsorption is possible. Together, the experimental results and analytical calculations support that DOCP lipid vesicle interactions with TiO_2 and SiO_2 surfaces depend on a combination of noncovalent and covalent forces in a distinct manner compared to previously studied vesicle systems where noncovalent forces alone predominate.

4. Discussion

It has long been recognized that vesicle adsorption behavior on inorganic surfaces such as SiO_2 and TiO_2 is dictated by noncovalent interfacial forces that influence the vesicle-surface interaction energy. In general, adsorbed vesicles undergo shape deformation that is influenced by an interplay of the membrane bending energy, deformation-related osmotic pressure energy, and vesicle-surface interaction energy [16, 38]. When the vesicle-surface interaction is repulsive, vesicle adsorption

will not occur. On the other hand, in cases of attractive but relatively weak vesicle-surface interactions, vesicles will adsorb but only exhibit modest adsorption-related deformation and remain intact on the surface. As vesicle-surface interactions become stronger, adsorbed vesicles will undergo greater deformation that can lead to spontaneous rupture due to a combination of vesicle-surface and vesicle-vesicle interactions. On TiO_2 surfaces, it is widely reported that adsorbed vesicles will remain intact while vesicles typically rupture to form an SLB on SiO_2 surfaces. These tendencies are attributed to the balance of interfacial forces underpinning vesicle-surface interactions and existing efforts to modulate vesicle adsorption behavior have focused on tuning the magnitudes of these noncovalent forces.

It is thus remarkable that, in spite of a large negative surface charge that imparts significant vesicle-surface charge repulsion, DOCP lipid vesicles can form SLB coatings on TiO_2 surfaces. From an interfacial engineering perspective, it is also important to understand the corresponding mechanistic details, especially determining the conditions in which SLB formation is possible along with the resulting functional properties such as antifouling capabilities. Indeed, trends in DOCP lipid vesicle interactions with TiO_2 nanoparticles in bulk solution have varied in past studies depending on the experimental assay and labeling conditions and reconciling different molecular-level perspectives could aid future application efforts. For example, when using lipid vesicles with a fluorescent membrane label, it was previously reported that DOCP lipid vesicles mainly adsorb onto TiO_2 nanoparticles at pH $<$ 7 whereas adsorption is inhibited pH $\geq$ 7 (Ref. [32]). On the other hand, when

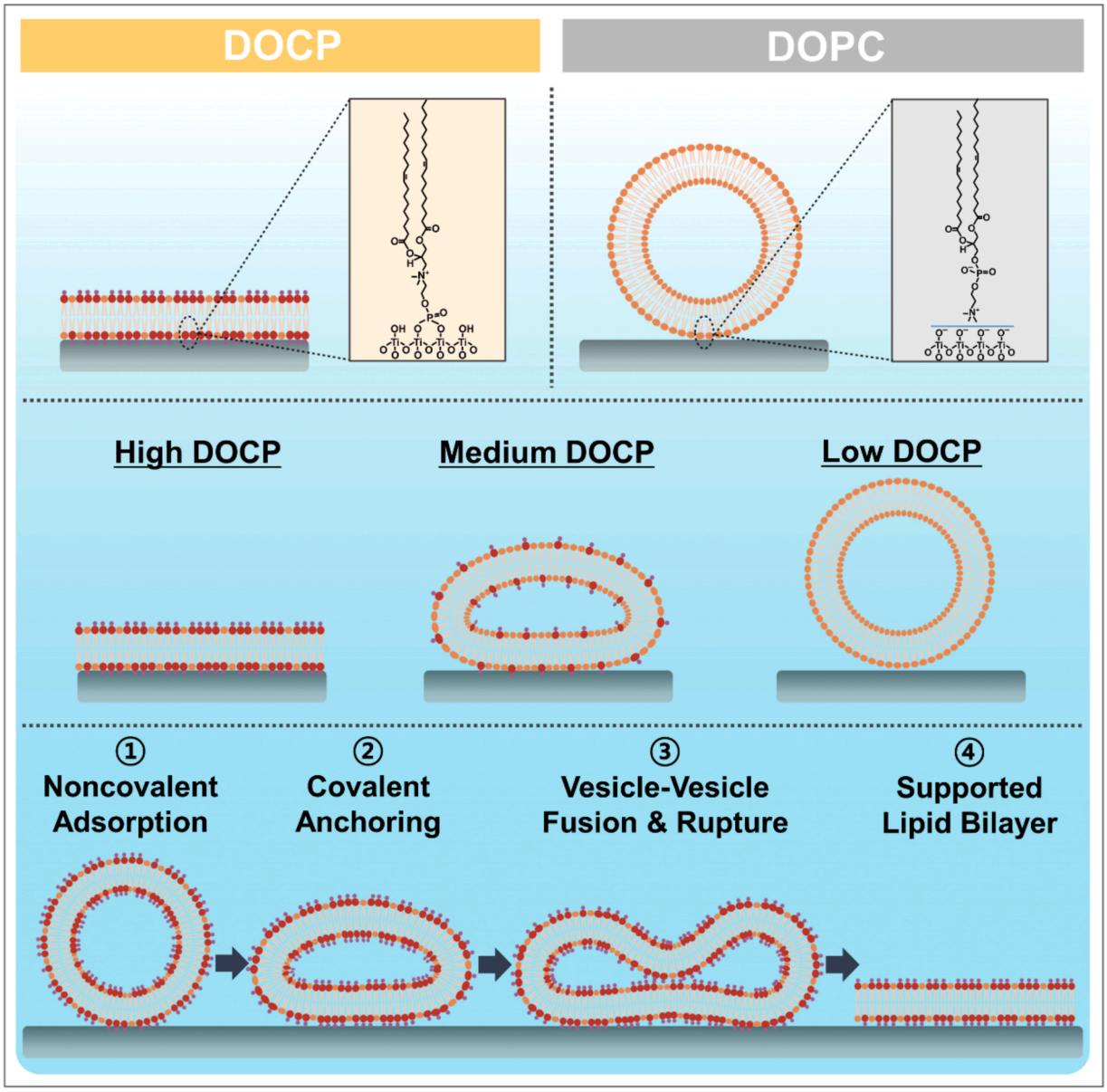

Fig. 5. Schematic summary of how noncovalent and covalent forces jointly contribute to DOCP lipid vesicle interactions with TiO_2 surfaces. Top: DOCP and DOPC lipid molecules mainly interact with TiO_2 surfaces though covalent bond formation and noncovalent adhesion, respectively. Middle: The interaction of DOCP-containing lipid vesicles with TiO_2 surfaces is affected by the DOCP fraction in the vesicles. At high DOCP fractions, supported lipid bilayer formation can occur due to strong vesicle-surface interactions while the interactions become progressively weaker at lower DOCP fractions. At intermediate DOCP fractions, vesicles adsorb and undergo deformation due to moderately strong interactions but do not rupture. At low DOCP fractions, vesicles adsorb but do not undergo extensive deformation due to relatively weak interactions. Bottom: Mechanism of how DOCP lipid vesicles interact with TiO_2 surfaces to form a supported lipid bilayer coating, which involves (1) noncovalent adsorption, (2) anchoring due to DOCP-TiO_2 covalent bond formation whereby greater bond density drives more extensive vesicle deformation, (3) fusion of deformed vesicles leading to rupture, and (4) lipid re-assembly to form a supported lipid bilayer.

measuring the release of water-soluble calcein dye from the interior of DOCP lipid vesicles without membrane label, it was determined that the vesicles can fuse with TiO_2 nanoparticles across pH 3, 7, and 10 (Ref. [35]).

By directly tracking the corresponding adsorption kinetics on a flat TiO_2 surface with the QCM-D technique, we focused on investigating the mechanistic details of how DOCP lipid vesicles form SLBs on TiO_2 surfaces, including both initial adsorption and fusion-related deformation and rupture, and identified that a combination of noncovalent and covalent forces is needed to drive the SLB formation process (Fig. 5). First, DOCP-containing lipid vesicles must have sufficiently favorable noncovalent interactions with TiO_2 surfaces to facilitate initial attachment. The attachment step is a prerequisite to facilitate bond formation between DOCP lipids and the TiO_2 surfaces – enabling the reactive moieties to come into sufficiently close contact – and requires suitable solution conditions, as evidenced by the 50 mM NaCl condition in which DOCP lipid vesicles did not adsorb. Second, DOCP lipid vesicles must form a sufficient density of covalent bonds with the TiO_2 surface to induce vesicle rupture. Strikingly, the presence of even 25 mol% DOCP lipids in a vesicle was shown to be insufficient to induce vesicle rupture; in that case, vesicles adsorbed and deformed to a greater extent than 100% mol DOPC lipid vesicles but did not rupture. In our experiments, at least 50 mol% DOCP lipids in a vesicle were necessary to induce vesicle rupture and SLB formation.

We analogize this dependency to multivalent ligand-receptor interactions involving ligand-modified vesicles and receptor-functionalized surfaces whereby greater multivalency translates into more extensive shape deformation [46] (see also other hybridization-related multivalent systems involving nucleic-acid-functionalized lipids [47–49]). We emphasize that DOCP-containing lipid vesicles appear to form covalent bonds – akin to anchoring points – with the TiO_2 surface in all applicable cases (as indicated by attached DOCP lipids after ethanol washing), but the variation in DOCP-TiO_2 bond density per vesicle (depending on the DOCP lipid fraction in the vesicles) determines the extent of vesicle deformation and hence whether attached vesicles remain intact or rupture to form an SLB. Hence, while DOCP-TiO_2 bond formation is necessary for SLB formation on TiO_2 surfaces, there are two additional key factors: (1) favorable conditions to facilitate noncovalent lipid vesicle adsorption onto the TiO_2 surface, otherwise, covalent bond formation cannot occur because lipid headgroups and the TiO_2 surface cannot come into sufficiently close proximity; and (2) a minimum density of DOCP-TiO_2 bonds, which we analogize to covalent anchoring points, in order to drive extensive vesicle deformation that can lead to fusion/rupture triggering SLB formation. While conventional vesicle fusion strategies involve enhancing noncovalent interactions to promote greater vesicle deformation, a unique aspect of the present system is that a combination of noncovalent and covalent forces is needed to drive DOCP-containing lipid vesicle fusion on TiO_2 surfaces. It should be noted that the attachment of DOCP-containing lipid vesicles to TiO_2 surfaces likely involves redistribution of lipids so that the DOCP lipid concentration in the vesicle-surface contact region is enhanced whereby a critical concentration is required to support deformation-mediated vesicle rupture.

Another striking feature is that, even for 100 mol% DOCP lipid vesicles where the highest possible density of covalent anchoring points can form, the QCM-D data indicate that vesicle-surface interactions are insufficient to cause rupture of individually attached vesicles and instead a combination of vesicle-surface and vesicle-vesicle interactions is needed to trigger the vesicle fusion and rupture process. This finding further highlights the distinct chemical features of DOCP lipid vesicle interactions on TiO_2 surfaces compared to more conventionally studied PC lipid vesicle interactions on SiO_2 surfaces where vesicle-surface interactions alone can induce rupture of individually attached vesicles, as dictated by noncovalent interfacial forces alone (especially electrostatic forces [50]). In marked contrast, DOCP-containing lipid vesicles are mainly repelled from SiO_2 surfaces due to extensive charge repulsion and, even in the limited cases where modest adsorption occurs, the extent of vesicle deformation is still insufficient to promote vesicle fusion/rupture. These observations highlight the importance of both noncovalent and covalent forces in utilizing DOCP lipid vesicles to form SLB coatings on inorganic surfaces such as TiO_2.

In terms of generalizing the fabrication concept, we may add a few additional remarks. First, we utilized DOPC/DOCP lipid vesicles in this study while it is likely possible to similarly modulate covalent and noncovalent forces using lipid vesicles composed of DOCP and other types of phospholipids. In order to support vesicle deformation, fluid-phase lipid properties are probably desirable while the hydration properties of the other lipids in the vesicle composition might also affect vesicle-surface interactions [51]. Second, the molecular geometry of the DOCP lipid molecule plays an important role in facilitating DOCP-TiO_2 bond formation because its phosphate group is presented outward and can readily form coordinate covalent bonds. Conversely, not all lipids that contain phosphate groups can bond with TiO_2 surfaces and hence the molecular design principles of the lipid headgroup are critical to support coordination. It might also be possible to design new lipid molecules that bear tethered phosphate groups to fabricate tethered lipid bilayer membranes on TiO_2 surfaces, for example [52].

5. Conclusion

In this work, we have demonstrated how balancing the interplay of noncovalent and covalent forces can tune the self-assembly pathway of DOCP lipid vesicles interacting with TiO_2 surfaces. Compared to other systems involving lipid vesicle interactions with inorganic surfaces, this system is unique in several respects. First, the noncovalent interactions between lipid vesicles and TiO_2 surfaces are relatively weak overall (likely due to steric-hydration repulsion [16,24]) and DOCP-TiO_2 covalent bond formation enables anchoring, which effectively serves as a potentiating force to enhance vesicle-surface interactions. Second, a minimum density of DOCP-TiO_2 covalent bonds – inferred from the DOCP fraction in vesicles – is needed to induce sufficiently high levels of vesicle deformation that can lead to fusion and rupture. At lower densities, covalent anchoring can still induce modest deformation of attached vesicles, but the vesicles do not fuse and rupture. Third, even at the highest DOCP fraction, vesicle-surface interactions by themselves are insufficient to drive rupture of individually attached vesicles on TiO_2 surfaces and instead a combination of vesicle-surface and vesicle-vesicle interactions is needed.

The latter observation demonstrates that the combination of noncovalent and covalent forces that drives DOCP lipid vesicle adsorption and rupture on TiO_2 surfaces is still relatively weak considering that noncovalent forces alone can induce sufficiently strong vesicle-surface interactions to rupture individually attached PC lipid vesicles on SiO_2 surfaces in some cases. As such, the interfacial chemistry underpinning DOCP lipid vesicle interactions with TiO_2 surfaces involves a subtle interplay of noncovalent and covalent forces and can induce SLB formation in select conditions. These findings also help to understand the interaction behavior of DOCP lipid vesicles with SiO_2 surfaces and more broadly highlight opportunities to modulate lipid self-assembly at inorganic surfaces by harnessing noncovalent and covalent forces in tandem, especially in cases involving coordination chemistry. These scientific insights can also enable engineering of more robust and tailored SLB platforms for various material science applications, especially in cases where firm attachment to the underlying substrate is needed along with antifouling capabilities. Such capabilities will also be aided by growing efforts to understand lipid bilayer properties using computational methods [53,54] and can potentially be applied to topics such as modulating cell-surface interactions [55].

Data availability

The raw data required to reproduce these findings are available from the corresponding authors on reasonable request.

CRediT authorship contribution statement

Tun Naw Sut: Conceptualization, Methodology, Investigation, Writing – original draft, Writing – review & editing. **Abdul Rahim Ferhan:** Investigation, Writing – review & editing. **Soohyun Park:** Investigation, Writing – review & editing. **Dong Jun Koo:** Investigation, Writing – review & editing. **Bo Kyeong Yoon:** Investigation, Writing – review & editing. **Joshua A. Jackman:** Conceptualization, Methodology, Investigation, Writing – original draft, Writing – review & editing, Supervision. **Nam-Joon Cho:** Conceptualization, Methodology, Investigation, Writing – original draft, Writing – review & editing, Supervision.

Declaration of Competing Interest

The authors declare no competing financial interest.

Acknowledgments

This work was supported by the National Research Foundation of Singapore through a Proof-of-Concept grant (NRF2015NRF-POC0001-19), by the Ministry of Education (MOE) in Singapore under Grant AcRF TIER1-2020-T1-002-032 (RG111/20), and by the National Research Foundation of Korea (NRF) grants funded by the Korean government (MSIT) (Nos. 2020R1C1C1004385, 2021R1A4A1032782, and 2022R1F1A1074690). In addition, this work was supported by the International Research & Development Program of the National Research Foundation of Korea (NRF) funded by the Ministry of Science and ICT (2020K1A3A1A39112724).

Supplementary materials

Supplementary material associated with this article can be found, in the online version, at doi:10.1016/j.apmt.2022.101618.

References

[1] E.T. Castellana, P.S. Cremer, Solid supported lipid bilayers: from biophysical studies to sensor design, Surf. Sci. Rep. 10 (2006) 429–444.
[2] R. Tero, Substrate effects on the formation process, structure and physicochemical properties of supported lipid bilayers, Materials 12 (2012) 2658–2680 (Basel).
[3] J. Liu, Interfacing zwitterionic liposomes with inorganic nanomaterials: surface forces, membrane integrity, and applications, Langmuir 18 (2016) 4393–4404.
[4] J.A. Jackman, N.J. Cho, Supported lipid bilayer formation: beyond vesicle fusion, Langmuir 6 (2020) 1387–1400.
[5] T.N. Sut, B.K. Yoon, W.Y. Jeon, J.A. Jackman, N.J. Cho, Supported lipid bilayer coatings: fabrication, bioconjugation, and diagnostic applications, Appl. Mater. Today (2021), 101183.
[6] M. Ramanathan, L.K. Shrestha, T. Mori, Q. Ji, J.P. Hill, K. Ariga, Amphiphile nanoarchitectonics: from basic physical chemistry to advanced applications, Phys. Chem. Chem. Phys. 26 (2013) 10580–10611.
[7] K. Ariga, S. Watanabe, T. Mori, J. Takeya, Soft 2D nanoarchitectonics, NPG Asia Mater. 4 (2018) 90–106.
[8] C. Keller, K. Glasmästar, V.P. Zhdanov, B. Kasemo, Formation of supported membranes from vesicles, Phys. Rev. Lett. 23 (2000) 5443.
[9] J.M. Johnson, T. Ha, S. Chu, S.G. Boxer, Early steps of supported bilayer formation probed by single vesicle fluorescence assays, Biophys. J. 6 (2002) 3371–3379.
[10] H. Schönherr, J.M. Johnson, P. Lenz, C.W. Frank, S.G. Boxer, Vesicle adsorption and lipid bilayer formation on glass studied by atomic force microscopy, Langmuir 26 (2004) 11600–11606.
[11] R.P. Richter, R. Bérat, A.R. Brisson, Formation of solid-supported lipid bilayers: an integrated view, Langmuir 8 (2006) 3497–3505.
[12] M. Mapar, S. Jõemetsa, H. Pace, V.P. Zhdanov, B. Agnarsson, F. Höök, Spatiotemporal kinetics of supported lipid bilayer formation on glass via vesicle adsorption and rupture, J. Phys. Chem. Lett. 17 (2018) 5143–5149.
[13] T.H. Anderson, Y. Min, K.L. Weirich, H. Zeng, D. Fygenson, J.N. Israelachvili, Formation of supported bilayers on silica substrates, Langmuir 12 (2009) 6997–7005.
[14] T.K. Lind, M. Cárdenas, Understanding the formation of supported lipid bilayers via vesicle fusion—a case that exemplifies the need for the complementary method approach, Biointerphases 2 (2016), 020801.
[15] M. Schneemilch, N. Quirke, Free energy of adsorption of supported lipid bilayers from molecular dynamics simulation, Chem. Phys. Lett. (2016) 199–204.
[16] E. Reimhult, F. Höök, B. Kasemo, Intact vesicle adsorption and supported biomembrane formation from vesicles in solution: influence of surface chemistry, vesicle size, temperature, and osmotic pressure, Langmuir 5 (2003) 1681–1691.
[17] V.P. Zhdanov, B. Kasemo, Comments on rupture of adsorbed vesicles, Langmuir 12 (2001) 3518–3521.
[18] M. Schneemilch, N. Quirke, Free energy of adhesion of lipid bilayers on silica surfaces, J. Chem. Phys. 19 (2018), 194704.
[19] M. Schneemilch, N. Quirke, Free energy of adhesion of lipid bilayers on titania surfaces, J. Chem. Phys. 13 (2019), 134707.
[20] K.H. Biswas, J.A. Jackman, J.H. Park, J.T. Groves, N.J. Cho, Interfacial forces dictate the pathway of phospholipid vesicle adsorption onto silicon dioxide surfaces, Langmuir 4 (2018) 1775–1782.
[21] E. Reimhult, F. Höök, B. Kasemo, Vesicle adsorption on SiO_2 and TiO_2: dependence on vesicle size, J. Chem. Phys. 16 (2002) 7401–7404.
[22] J.A. Jackman, B. Špačková, E. Linardy, M.C. Kim, B.K. Yoon, J. Homola, N.J. Cho, Nanoplasmonic ruler to measure lipid vesicle deformation, Chem. Commun. 1 (2016) 76–79.
[23] A.R. Ferhan, B. Spackova, J.A. Jackman, G.J. Ma, T.N. Sut, J. Homola, N.J. Cho, Nanoplasmonic ruler for measuring separation distance between supported lipid bilayers and oxide surfaces, Anal. Chem. 21 (2018) 12503–12511.
[24] J.A. Jackman, G.H. Zan, Z. Zhao, N.J. Cho, Contribution of the hydration force to vesicle adhesion on titanium oxide, Langmuir 19 (2014) 5368–5372.
[25] N.J. Cho, J.A. Jackman, M. Liu, C.W. Frank, pH-driven assembly of various supported lipid platforms: a comparative study on silicon oxide and titanium oxide, Langmuir 7 (2011) 3739–3748.
[26] A. Kunze, P. Sjövall, B. Kasemo, S. Svedhem, *In situ* preparation and modification of supported lipid layers by lipid transfer from vesicles studied by QCM-D and TOF-SIMS, J. Am. Chem. Soc. 7 (2009) 2450–2451.
[27] F.F. Rossetti, M. Bally, R. Michel, M. Textor, I. Reviakine, Interactions between titanium dioxide and phosphatidyl serine-containing liposomes: formation and patterning of supported phospholipid bilayers on the surface of a medically relevant material, Langmuir 14 (2005) 6443–6450.
[28] A.R. Ferhan, B.K. Yoon, S. Park, T.N. Sut, H. Chin, J.H. Park, J.A. Jackman, N. J. Cho, Solvent-assisted preparation of supported lipid bilayers, Nat. Protoc. (2019) 2091–2118.
[29] S.R. Tabaei, J.A. Jackman, S.O. Kim, V.P. Zhdanov, N.J. Cho, Solvent-assisted lipid self-assembly at hydrophilic surfaces: factors influencing the formation of supported membranes, Langmuir 10 (2015) 3125–3134.
[30] Y. Liu, F. Wang, J. Liu, Headgroup-inversed liposomes: biointerfaces, supported bilayers and applications, Langmuir 32 (2018) 9337–9348.
[31] E.K. Perttu, A.G. Kohli, F.C. Szoka Jr, Inverse-phosphocholine lipids: a remix of a common phospholipid, J. Am. Chem. Soc. 10 (2012) 4485–4488.
[32] F. Wang, J. Liu, A stable lipid/TiO_2 interface with headgroup-inversed phosphocholine and a comparison with SiO_2, J. Am. Chem. Soc. 36 (2015) 11736–11742.
[33] F. Wang, X. Zhang, Y. Liu, Z.Y. Lin, B. Liu, J. Liu, Profiling metal oxides with lipids: magnetic liposomal nanoparticles displaying DNA and proteins, Angew. Chem. Int. Ed. 39 (2016) 12063–12067.
[34] S.P. Pujari, L. Scheres, A.T.M. Marcelis, H. Zuilhof, Covalent surface modification of oxide surfaces, Angew. Chem. Int. Ed. 25 (2014) 6322–6356.
[35] X. Wang, X. Li, H. Wang, X. Zhang, L. Zhang, F. Wang, J. Liu, Charge and coordination directed liposome fusion onto SiO_2 and TiO_2 nanoparticles, Langmuir 5 (2019) 1672–1681.
[36] R.C. MacDonald, R.I. MacDonald, B.P.M. Menco, K. Takeshita, N.K. Subbarao, L. R. Hu, Small-volume extrusion apparatus for preparation of large, unilamellar vesicles, Biochim. Biophys. Acta Biomembr. 2 (1991) 297–303.
[37] N.J. Cho, C.W. Frank, B. Kasemo, F. Höök, Quartz crystal microbalance with dissipation monitoring of supported lipid bilayers on various substrates, Nat. Protoc. 6 (2010) 1096–1106.
[38] J.A. Jackman, J.H. Choi, V.P. Zhdanov, N.J. Cho, Influence of osmotic pressure on adhesion of lipid vesicles to solid supports, Langmuir 36 (2013) 11375–11384.
[39] J.A. Jackman, Z. Zhao, V.P. Zhdanov, C.W. Frank, N.J. Cho, Vesicle adhesion and rupture on silicon oxide: influence of freeze–thaw pretreatment, Langmuir 30 (2014) 2152–2160.
[40] B. Seantier, B. Kasemo, Influence of mono- and divalent ions on the formation of supported phospholipid bilayers via vesicle adsorption, Langmuir 10 (2009) 5767–5772.
[41] C.A. Keller, B. Kasemo, Surface specific kinetics of lipid vesicle adsorption measured with a quartz crystal microbalance, Biophys. J. 3 (1998) 1397–1402.
[42] S.R. Tabaei, J.H. Choi, G.H. Zan, V.P. Zhdanov, N.J. Cho, Solvent-assisted lipid bilayer formation on silicon dioxide and gold, Langmuir 34 (2014) 10363–10373.
[43] V.V. Murashov, J. Leszczynski, Adsorption of the phosphate groups on silica hydroxyls: an *ab initio* study, J. Phys. Chem. A 9 (1999) 1228–1238.
[44] L. Cai, Q. Sun, M. Bao, H. Ma, C. Yuan, W. Xu, Competition between hydrogen bonds and coordination bonds steered by the surface molecular coverage, ACS Nano 4 (2017) 3727–3732.
[45] S. Sun, C. Liu, D.R. Melendez, T. Yang, P.S. Cremer, Immobilization of phosphatidylinositides revealed by bilayer leaflet decoupling, J. Am. Chem. Soc. 30 (2020) 13003–13010.

[46] H. Park, T.N. Sut, B.K. Yoon, V.P. Zhdanov, N.J. Cho, J.A. Jackman, Unraveling how multivalency triggers shape deformation of sub-100nm lipid vesicles, J. Phys. Chem. Lett. 28 (2021) 6722–6729.
[47] M. Chung, R.D. Lowe, Y.H.M. Chan, P.V. Ganesan, S.G. Boxer, DNA-tethered membranes formed by giant vesicle rupture, J. Struct. Biol. 1 (2009) 190–199.
[48] M. Chung, S.G. Boxer, Stability of DNA-tethered lipid membranes with mobile tethers, Langmuir 9 (2011) 5492–5497.
[49] M. Chung, B.J. Koo, S.G. Boxer, Formation and analysis of topographical domains between lipid membranes tethered by DNA hybrids of different lengths, Faraday Discuss. 161 (2013) 333–345.
[50] J.A. Jackman, N.J. Cho, R.S. Duran, C.W. Frank, Interfacial Binding dynamics of bee venom phospholipase A_2 investigated by dynamic light scattering and quartz crystal microbalance, Langmuir 6 (2010) 4103–4112.
[51] V. Wieser, L.L.E. Mears, R.D. Barker, H.W. Cheng, M. Valtiner, Hydration forces dominate surface charge dependent lipid bilayer interactions under physiological conditions, J. Phys. Chem. Lett. 12 (2021) 9248–9252.
[52] J.A. Jackman, W. Knoll, N.J. Cho, Biotechnology applications of tethered lipid bilayer membranes, Materials 5 (2012) 2637–2657.
[53] M.I. Mahmood, T. Yamashita, Influence of lipid bilayer on the GPCR structure: comparison of all-atom lipid force fields, Bull. Chem. Soc. Jpn. 94 (2021) 2569–2574.
[54] Y. Zhang, P.M. Dijkman, R. Zou, M. Zandl-Lang, R.M. Sanchez, L. Eckhardt-Strelau, H. Köfeler, H. Vogel, S. Yuan, M. Kudryashev, Asymmetric opening of the homopentameric 5-HT_{3A} serotonin receptor in lipid bilayers, Nat. Commun. 12 (2021) 1074.
[55] X. Jia, J. Song, W. Lv, J.P. Hill, J. Nakanishi, K. Ariga, Adaptive liquid interfaces induce neuronal differentiation of mesenchymal stem cells through lipid raft assembly, Nat. Commun. 13 (2022) 1074.